Planar Ferrite Isolator Combining Edge-Guided Mode and Gyro-Resonance Absorption

S. Khim[#$], T. Monediere[#], H. Parvery[$], B. Frigui[$], D. Passerieux[#], J.L. Valdes[#], L. Huitema[#*]
[#]XLIM, UMR CNRS 7252, University of Limoges, France
[$]CISTEME, France
[*]Institut Universitaire de France (IUF), France
{sokha.khim, thierry.monediere, jehison.leon-valdes, laure.huitema}@unilim.fr,
damien.passerieux@xlim.fr, {parvery, frigui}@cisteme.net

2026 IEEE MTT-S Radio Frequency Technology and Techniques Symposium (IMS RFTT) | 979-8-3315-4766-0/26/$31.00 ©2026 IEEE | DOI: 10.1109/IMSRFTT43070.2026.11602538

***Abstract*— This work presents a planar microstrip ferrite isolator that utilizes both the phenomenon of edge-guided propagation and that of absorption due to gyromagnetic resonance. Nonreciprocal transmission is realized through asymmetric stub perturbations, eliminating the need for lossy absorbers or shorted strips and enabling compact, low-cost fabrication. Simulations and measurements confirm low insertion losses of less than 0.9 dB, combined with isolation and reflection coefficients greater than 20 dB over a fractional bandwidth of approximately 11%. Compared to conventional edge-guided or resonance-based designs, the proposed hybrid approach improves backward-to-forward loss ratio while maintaining a simple planar implementation, providing a practical path toward highly performance, integrable nonreciprocal microwave components.**

***Keywords*—Ferrite, isolator, edge-guided mode, ferrimagnetic resonance, non-reciprocal device, field displacement.**

I. Introduction

Ferrite isolators are key nonreciprocal components that ensure unidirectional signal transmission, suppress reflections, and protect sensitive RF circuitry. They are vital in radar and satellite communication systems, where low loss, high isolation, and compact integration are critical requirements [1]. Many conventional designs appear in the literature. Traditional Y-junction circulator-based isolators, although robust and reliable, tend to be bulky and require an external termination load. This load is typically connectorized and cumbersome, making system integration challenging. A 3D-printed microstrip circulator-based isolator reported in [2] achieved comparable isolation and insertion loss to conventional devices but required complex multi-material printing and ferrite embedding, which limit fabrication simplicity and scalability.

Resonance isolators achieve nonreciprocal transmission by exploiting ferrite losses near gyromagnetic resonance, as reported in [3], [4], [5], [6]. In [5], planar resonance isolators provided convincing isolation bandwidth, however they required a strong bias field, and involved inconvenient ferrite loading. A miniaturized microstrip resonance isolator [6] demonstrated a new ferrite polarization mechanism along the propagation direction. It suffered from high insertion loss (3.5 dB). A relatively strong magnetic field (4 kOe), and therefore probably heavy and bulky magnets, is required on part of that frequency band. A promising isolator concept is the edge-guided mode (EGM), which exploits the asymmetric deformation of the electromagnetic field in a ferrite-loaded microstrip line magnetized perpendicularly to the propagation direction, with isolation achieved through asymmetric edge loading. The first designs relied on asymmetric absorber loading to suppress backward wave [7]. A subsequent version introduced in [8] replaced lossy material with wide strip shorted to ground, achieving a higher backward-to forward loss ratio but requiring grounding structures.

In [9], a ferrite-filled rectangular waveguide isolator using inkjet printing is reported. The isolation is achieved by applying an anti-symmetrical DC magnetic bias to the ferrite-filled waveguide. The inkjet-printed metallization offered design flexibility but 4 dB insertion loss due to silver resistivity and imperfect magnetization of the ferrite.

A design using short-circuited microstrip lines is presented in [10]. It has further improved rear wave suppression by using two antiparallel magnetized ferrites (requiring two magnets) and also two short circuits. This makes implementation more difficult. A wideband, two-octave cryogenic edge-guided stripline isolator developed for radio astronomy in [11] achieved less than 1 dB insertion loss but required long tapered and curved strip with lossy absorbers, resulting in large footprint ($1.1\lambda_0 \times 1.37\lambda_0$) & high cost. Hybrid design that combines resonance absorption and EMG [12] have been explored. However, their complex biasing and shorted-strip structures continue to pose challenges for practical realization.

A planar ferrite isolator that merges EGM propagation with resonance absorption in a single ferrite structure is presented in this work. Asymmetrical stubs perturbations selectively suppress backward waves, while a single permanent magnet produces a nonuniform bias field enabling low-loss forward transmission and strong reverse attenuation. This design achieves high isolation without absorbers or short circuits, offering a fractional bandwidth (11%), low insertion loss (0.81 dB), and simple, low-cost fabrication suitable for integrated nonreciprocal, compact microwave systems.

II. Theory of Edge-Guided Mode

The non-reciprocal behavior of a ferrite biased by a continuous (DC) magnetic field enough to saturate is characterized by the Polder permeability tensor [13].

$$[\mu_r(\omega)] = \begin{bmatrix} \mu & -j\kappa & 0 \\ j\kappa & \mu & 0 \\ 0 & 0 & 1 \end{bmatrix} \quad (1)$$

Authorized licensed use limited to: Universite De Limoges. Downloaded on October 01,2026 at 13:36:41 UTC from IEEE Xplore. Restrictions apply.

Another essential parameter for modeling the behavior of the material is its effective permeability.

$$\mu_{eff} = \mu - \frac{\kappa^2}{\mu^2}. \quad (2)$$

Where, tensor elements (μ & κ) are calculated by: $\mu = 1 + (\omega_m\omega_0/(\omega_0^2 - \omega^2))$ and $\kappa = \omega_m\omega/(\omega_0^2 - \omega^2)$. If the magnetic loss included, the Larmor pulsation frequency is given by $\omega_0 = \gamma H_{in} + j\omega\alpha$. And, $\omega = 2\pi f$, $\omega_m = 2\gamma\pi M_s$ are operating frequency and magnetization frequency, respectively. Moreover, $\gamma = 2.8$ MHz/Oe is the gyromagnetic ratio. Whilst, α is the damping factor.

When a wide microstrip line on a ferrite substrate is magnetized perpendicularly to the ground plane, and when the effective permeability of the material (μ_{eff}) is negative the energy propagates along one edge, forming the so-called edge-guided mode [7], [8], [9], [10], [11]. Fig. 1(a) illustrates this phenomenon which was first explained analytically M.E. Hines [7]. Indeed, the design begins by selecting the ferrite's saturation magnetization, followed by defining an appropriate internal biasing field that aligns the operating frequency (f) within the span of negative-permeability plot of μ_{eff}. The higher the saturation the wider the operating band of EGM. Moreover, the edge-guided mode electric and magnetic field are reported to be exponential decay in [7], [14]. In [14], simplified electric (E_z) and magnetic (H_x) fields are given by (3) & (4):

$$E_z = A_c \frac{\omega\mu_0\mu_{eff}s}{s\beta_{EG}\mu - \kappa\alpha_{EG}} e^{s\alpha_{EG}x} e^{-j\beta_{EG}y} \quad (3)$$

$$H_x = A_c e^{s\alpha_{EG}x} e^{-j\beta_{EG}y}. \quad (4)$$

A_c is the amplitude of the field component. And, the factor (s) equals $s = \kappa\beta_{EG}/|\kappa\beta_{EG}|$ which edge mode phase constant (β_{EG}) given by $\beta_{EG} = \omega/c\sqrt{\mu\varepsilon_f}$. The attenuation constant of edge mode (α_{EG}) is estimated by $\alpha_{EG} = |\kappa\beta_{EG}/\mu|$. These fields depend on Polder Tensor elements μ, κ, and μ_{eff}. And, $c = 3 \times 10^8$ (m/s) is the speed of light in vacuum. The spatial coordinates x and y correspond to the width and length of the microstrip line, respectively.

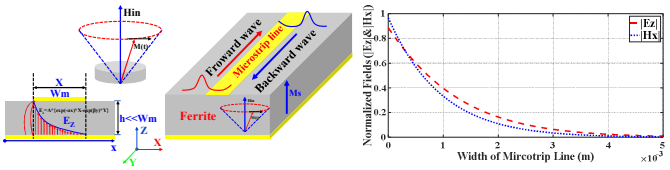

(a) (b)

Fig. 1. (a) Modelling of EMG microstrip. (b) Plot of normalized exponential fields profile of EMG.

In this work, a commercial ferrite Y210 is used. It has low magnetic loss of ΔH_{eff}=2 Oe, high permittivity ε_r=14.2 and saturation magnetization $4\pi M_s$ =1000 G. An effective permeability ($\mu_{eff} = -2.2$) is calculated using (2) at 2.5 GHz for an internal field H_{in}=300 Oe. This calculation ensures isolator functions in the fundamental edge-guided mode. With the same ferrite properties, internal biasing field, and a 5.5 mm-wide microstrip line, the normalized electric and magnetic field distributions are calculated using (3) & (4), plotted in Fig. 1(b).

III. Perturbation of Resonance and Edge-Guided Mode Isolators

Resonance isolators leverage ferrite losses near gyromagnetic resonance to achieve nonreciprocal absorption. Planar resonance isolators using substrate integrated waveguide (SIW) technology improve integration potential are presented in [5]. Fig. 2(a) illustrates the case where the backward energy is absorbed by a ferrite slab working near the gyromagnetic resonance. Indeed, ferrite-loaded is challenged fabrication and tradeoff, as isolation performance is highly sensitive to ferrite slab dimensions and often deteriorates insertion loss.

In previous section, in magnetized ferrite microstrip line, energy naturally concentrates along one edge at frequencies where μ_{eff} <0, forming an edge-guided mode. Isolation is conceived by mean of perturbation on one side of the edge-guided mode. The perturbation in this work was built on our previous works [15], [16]. At first, we solved a drawbacks of high magnetic loss ferrite and then proposed novel asymmetrical stubs perturbation In this work, asymmetrical stubs perturbations are further refined through Gyro-resonance, enabling reverse-wave suppression without affecting the forward transmission. Implemented on a single ferrite substrate, this approach preserved low forward loss while delivering higher isolation (see Fig. 2(b)). Together, this work established a practical pathway toward miniature, cost-effective, and integration-friendly edge-guided mode isolator without absorber or shorted strips.

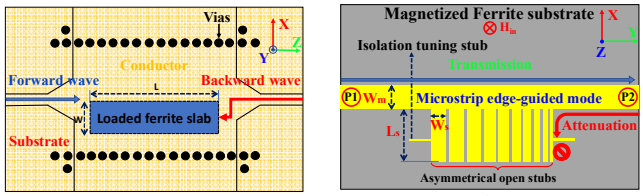

(a) (b)

Fig. 2. (a) Top view of E-plane resonance isolator [5]. (b) Proposed microstrip edge-guided mode isolator with asymmetrical stubs.

IV. Fusion of Resonance and Edge-Guided Modes

A. Working Principles

This work proposes the design of an isolator combining the effects of two phenomena: edge-guided mode and resonance absorption (Fig. 3(a)). The first allows for optimal transmission (with low losses) in the forward direction. The second prevents reverse propagation and ensures good isolation. This hybrid approach merges the advantages of compactness, broader operation, and strong isolation, while mitigating the drawbacks of earlier design [16]. A ferrite Y210 ($4\pi M_s$=1000 G, ε_r=14.2) was used and modelized using Polder tensor as illustrated in Fig. 3(b).

In this study, a weaker bias field $H_{in1} = 300$ Oe beneath the main line supports low-loss forward transmission, while a stronger bias $H_{in2} = 1000$ Oe beneath stubs drives gyromagnetic resonance at 2.8 GHz, selectively absorbing the backward wave. Impedance matching (via a quarter-wave transformer) is performed to enable measurement as depicted in Fig. 3(a).

Authorized licensed use limited to: Universite De Limoges. Downloaded on October 01,2026 at 13:36:41 UTC from IEEE Xplore. Restrictions apply.

This hybridization, validated through full-wave CST electromagnetic (EM) simulations, delivers a 10.5% bandwidth around 2.68 GHz, with isolation and matching better than 20 dB, and insertion loss lower than 0.3 dB (Fig. 3(c)). As observed, the EGM alone achieves only about half the bandwidth for similar loss levels. These results highlight the potential.

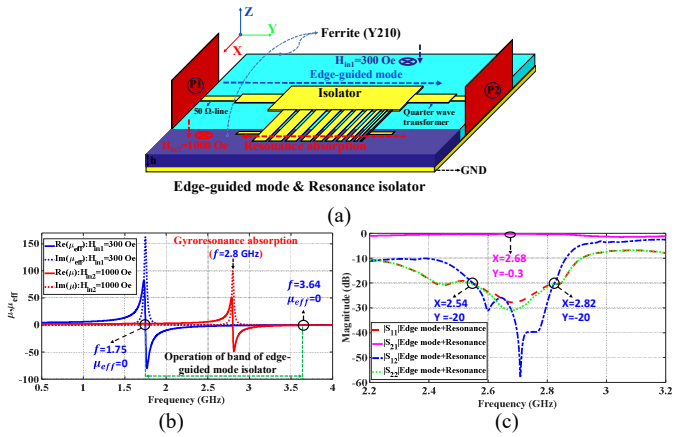

Fig. 3. (a) Modelling of hybrid isolator. (b) Plot of permeabilities for ferrite Y210 vs. frequency: effective permeability (μ_{eff}): H_{in1} =300 Oe (blue) and permeability (μ): H_{in2}=1000 Oe (red). (c) S-parameter of proposed isolator.

B. *Exploiting Co-simulation and External Biasing Scheme*

Previous simulations assumed a homogeneous internal magnetic field, which does not accurately represent the polarization produced by permanent magnet. To model realistic conditions, a magnetostatic (MS) simulation was performed in CST to effectively determine the internal biasing fields inside the ferrite. Unlike conventional approaches that rely solely on a single mechanism, our method creates two phenomena within the same ferrite substrate using a single samarium cobalt (SmCo5-18MGO) permanent magnet which has remanent magnetic flux density (B_r=0.88 T). The two desired magnetic field values ($H_{in1} \approx$ 300 Oe under the microstrip line and $H_{in2} \approx$1000 Oe under the asymmetrical stubs) are obtained using a single permanent magnet.

The cross-sectional view of the proposed co-simulation, illustrated in Fig. 4(a) shows that it is possible to achieve these biasing conditions by introducing a lateral offset of the overall isolator relative from the center of the magnet.

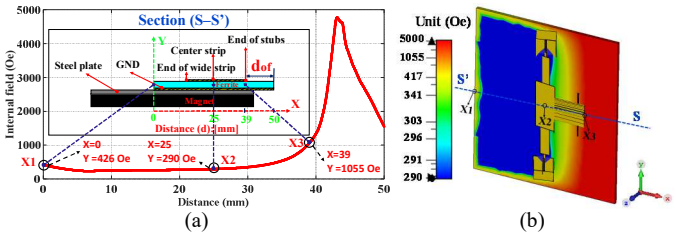

Fig. 4. (a) Biasing field distribution inside ferrite (co-simulation) with magnet (SmCo5-18MGO), Br = 0.88 T. (b) Magnitude of H-field inside isolator.

Indeed, magnetostatics analysis reveals that the magnet naturally generates stronger fields near its edges than at its center. This gradient is exploited by shifting the ferrite along the x-axis. The resulting internal field distribution that maps the plotting, illustrated in Fig. 4(b), confirms that the required dual-field biasing can be obtained with an optimized offset of 11 mm. This approach provides a practical, low-cost implementation of non-uniform biasing, simplifying implementation while preserving the enhanced performance predicted by full-wave simulations.

V. Implementation and Experimental Results

To experimentally validate the proposed concept, a prototype isolator was fabricated on a ferrite substrate (50 × 50 × 1 mm³). The magnetic biasing was provided by samarium-cobalt permanent magnet with steel plate or pole piece to improve homogenous field biasing, placed in between. The assembled device was housed in a low-permittivity Rohacell box ($\varepsilon_r \approx 1$) which ensured stable access to the measuring probe Fig. 5(a).

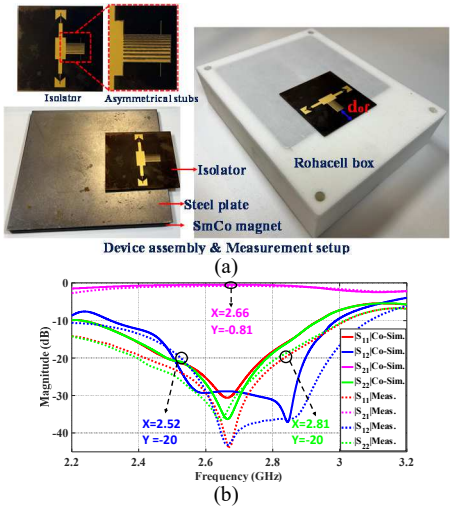

Fig. 5. (a) Fabrication of isolator. (b) Simulated (solid lines) Vs. measured (dot lines) results.

Each piece was assembled and measurements were taken using a 125 μm pitch cascade probe (GSG) from MPI Corporation. The measurement results are shown in Fig. 5(b). Comparison between co-simulation and measurements, demonstrates a good agreement. The isolator gives a 10.9% fractional bandwidth (2.52–2.81 GHz) with $|S_{12}|$, $|S_{11}|$, and $|S_{22}|$ all greater than 20 dB, a peak isolation of 43 dB, and minimum insertion loss of 0.81 dB at 2.66 GHz.

Table 1. Compared to the literatures

Ref.	Type	ǂBW$_{R\&I}$ (%)	×$\|S_{21}\|$ (dB)	Fabrication & Sys. Int.	F_c (GHz)	Length (λ_0)
[2]	3D-printed isolator	0.0	0.76	Hard & Yes	6.14	$0.9\lambda_0$
[5]	SIW Resonance	!0.0	!1.1	Hard & Yes	10.02	≈$0.93\lambda_0$
		*6.1	*2.3		10.09	
[9]	Edge-guided mode	0.0	2.73	Hard & Yes	10.8	$1.18\lambda_0$
[10]	Edge-guided mode	4.8	1.3	Hard & No	6.25	$0.84\lambda_0$
[11]	Edge-guided mode	112	0.9	Hard & No	9.5	$1.37\lambda_0$
[12]	Edge-guided and resonance	0.0	1	Hard & No	6	$0.89\lambda_0$
T. W	Edge-guided and resonance	10.9	0.81	Easy & Yes	2.66	$0.44\lambda_0$

ǂBW$_{R\&I}$= BW of $|S_{11}|$ or $|S_{22}|$ & $|S_{12}|$>20 dB; ×$|S_{21}|$ low insertion loss; !E-plane load; *Surface loaded; Sys. Int.=system integrated. T. W=this work

Authorized licensed use limited to: Universite De Limoges. Downloaded on October 01,2026 at 13:36:41 UTC from IEEE Xplore. Restrictions apply.

The measured results confirm strong isolation with low insertion loss. The fractional bandwidth is narrower than that of classical edge-guided mode isolators due to the nature of stubs. Although bandwidth could be increased by additional absorber loading or grounding vias, this would increase footprint and fabrication complexity. The slightly variation in reflection bandwidth and isolation in measured are attributed to a minor offset of the permanent magnet, which alters the internal bias field relative to the intended co-simulation configuration. Our design instead prioritizes compact size and simplified implementation.

Table 1 compares the performance of the proposed isolator with those reported in the literature. The 3D-printed isolator/circulator achieved excellent insertion loss (0.76 dB), but negligible usable bandwidth ($BW_{R\&I}$) and significant form factors. Furthermore, the use of adhesive copper makes it difficult to use in industrial applications [2]. The SIW resonance isolators [5], demonstrated good PCB compatibility and scalability potential, yet their surface ferrite-loaded structure exhibited more insertion loss (2.3 dB) and limited usable bandwidth (6.1%), while E-plane loading reduced loss but introduced severe mismatch. The inkjet-printed edge-guided mode isolator [9] demonstrated progress in additive manufacturing and integration but suffered from incomplete ferrite magnetization under dual-magnet biasing, yielding 2.73 dB insertion loss and ~16 dB reflection at port 2. The microstrip design in [10] refined the approach in [9], lowering loss to 1.3 dB and expanding the $BW_{R\&I}$ to 4.8%, though fabrication and biasing remained complex. In [11], the ultra-broadband design achieved remarkable isolation bandwidth (>100%) and low loss (<1 dB). Nonetheless, it required the use of complex absorber assemblies and exhibited poor port 2 matching with an extended footprint of $1.37\lambda_0$. A hybrid edge-guided and resonant absorption stripline isolator [12], achieved less than 1 dB loss and wide reflection matching. However, the design relied on a vertically mounted soft steel plate ($40 \times 7 \times 1$) mm near short-circuiting wall to generate a strong local DC bias field, restricting integration feasibility. Our isolator achieves low insertion loss (less than 0.9 dB), isolation, and matching better than 20 dB over a bandwidth of 10.9% centered at 2.66 GHz with a compact planar form with a length of only $0.44\lambda_0$.

VI. Conclusion

This paper presents the original design of a compact ferrite microstrip isolator that combines edge-guide mode and resonance absorption phenomena. The ferrite is polarized by a single permanent magnet that is carefully positioned. The novel stub perturbation enables a compact footprint while strategically biasing allows isolator to operate in other phenomena. This facilitates manufacturability and integration capability, and offers a practical pathway toward compact co-integrated microwave subsystems.

Acknowledgment

This work was supported and funded by L'Agence de l'Innovation de la Défense (AID) et l'Agence Nationale de la Recherche (ANR) as part of the CAFE project:(ANR-24-ASTR-0019). It was carried out at the INOGYRO joint laboratory between the SME Inoveos and the XLIM research institute (https://inogyro.xlim.fr/). The circuit etching was carried out at Inoveos (LPKF ProtoLaser U4). All or part of the experiments were carried out at the PLATINOM test platform at XLIM, a member of the CNRS RF-Net network.

References

[1] V. G. Harris, *Modern Ferrites, Volume 2: Emerging Technologies and Applications*. in IEEE Press. Wiley, 2022.

[2] V. Laur, J. P. Gouavogui, and B. Balde, "C-Band Hybrid 3-D-Printed Microwave Isolator," *IEEE Trans. Microwave Theory Techn.*, vol. 69, no. 3, pp. 1579–1585, Mar. 2021, doi: 10.1109/TMTT.2021.3053277.

[3] L. Lewin, "A resonance absorption isolator in microstrip for 4 Gc/s," *Proceedings of the IEE-Part B: Radio and Electronic Engineering*, vol. 6, no. 104, pp. 364–365, 1957.

[4] M. Noferesti and T. Djerafi, "A Tunable Ferrite Isolator for 30 GHz Millimeter-Wave Applications," *IEEE Transactions on Magnetics*, vol. 57, no. 7, pp. 1–7, Jul. 2021.

[5] Y. J. Cheng, Q. D. Huang, Y. R. Wang, and J. L.-W. Li, "Narrowband Substrate Integrated Waveguide Isolators," *IEEE Microw. Wireless Compon. Lett.*, vol. 24, no. 10, pp. 698–700, Oct. 2014.

[6] J. Wu, M. Li, X. Yang, S. Beguhn, and N. X. Sun, "A Novel Tunable Planar Isolator with Serrated Microstrip Structure," *IEEE Trans. Magn.*, vol. 48, no. 11, pp. 4371–4374, Nov. 2012.

[7] M.E. Hines, "Reciprocal and Nonreciprocal Modes of Propagation in Ferrite Stripline and Microstrip Devices," *IEEE Transactions on Microwave Theory and Techniques*, vol. 19, no. 5, pp. 442–451, May 1971.

[8] K. Araki, T. Koyama, and Y. Naito, "Reflection Problems in a Ferrite Stripline," *IEEE Trans. Microwave Theory Techn.*, vol. 24, no. 8, pp. 491–498, Aug. 1976, doi: 10.1109/TMTT.1976.1128886.

[9] M. F. Farooqui, A. Nafe, and A. Shamim, "Inkjet printed ferrite-filled rectangular waveguide X-band isolator," in *2014 IEEE MTT-S International Microwave Symposium*, IEEE, Jun. 2014, pp. 1–4.

[10] W. Marynowski, "Integrated Broadband Edge-Guided Mode Isolator With Antiparallel Biasing of the Ferrite Slabs," *IEEE Microw. Wireless Compon. Lett.*, vol. 28, no. 5, pp. 392–394, May 2018.

[11] L. Zeng, C.-Y. E. Tong, and S. N. Paine, "A Low-Insertion Loss Cryogenic Edge-Mode Isolator With 18 GHz Bandwidth," *IEEE Journal of Microwaves*, vol. 3, no. 4, pp. 1258–1266, Oct. 2023, doi: 10.1109/JMW.2023.3307297.

[12] T. Noguchi, "New Edge-Guided Mode Isolator Using Ferromagnetic Resonance Absorption," *IEEE Transactions on Microwave Theory and Techniques*, vol. 25, no. 2, pp. 100–106, Feb. 1977, doi: 10.1109/TMTT.1977.1129048.

[13] J. D. Adam, L. E. Davis, G. F. Dionne, E. F. Schloemann, and S. N. Stitzer, "Ferrite devices and materials," *IEEE Trans. Microwave Theory Techn.*, vol. 50, no. 3, pp. 721–737, Mar. 2002, doi: 10.1109/22.989957.

[14] T. Ueda and M. Tsutsumi, "Nonreciprocal left-handed transmission characteristics of microstriplines on ferrite substrate," *IET Microw. Antennas Propag.*, vol. 1, no. 2, p. 349, 2007, doi: 10.1049/iet-map:20050006.

[15] S. Khim, J. L. Valdes, H. Parvery, L. Huitema, and T. Monediere, "Planar Isolator Based on Field Displacement in Ferrite Substrate," in *2024 54th European Microwave Conference (EuMC)*, Sep. 2024, pp. 172–175. doi: 10.23919/EuMC61614.2024.10732277.

[16] S. Khim *et al.*, "Novel Topology of Reversed Wave Attenuation in Microstrip Ferrite Edge-Guided Mode Isolator," *IEEE Microwave and Wireless Technology Letters*, pp. 1–4, 2026, doi: 10.1109/LMWT.2026.3651400.

Authorized licensed use limited to: Universite De Limoges. Downloaded on October 01,2026 at 13:36:41 UTC from IEEE Xplore. Restrictions apply.